sustainability

MDPI

Article

Mechanical Performance and Low-Carbon Sustainability of Cement-Stabilized Macadam with Recycled Plastic Aggregate

Haijun Guo [1,2], Mingxiang Chi [1], Shibin Chen [1,*], Yunshi Yao [1], Weidong Guo [1] and Chuanqiang Chen [1]

[1] Key Laboratory of Road Construction Technology and Equipment of MOE, Chang'an University, Xi'an 710064, China; guohj@chd.edu.cn (H.G.)
[2] Modern Engineering Training Center, Chang'an University, Xi'an 710064, China
* Correspondence: sbchen@chd.edu.cn

Abstract

Against the background of the global "dual carbon" strategic goal, low-carbon upgrading of road engineering and efficient recycling of waste plastics have become critical approaches to relieve the shortage of natural aggregates and control plastic pollution. Most existing studies only focus on the optimization of single mechanical indicators, while lacking collaborative analysis of mechanical performances and carbon reduction benefits, meaning they cannot provide sufficient scientific support for the design of low-carbon and sustainable road materials. In this study, recycled plastic aggregate (PA) was used to partially replace natural coarse aggregate, and its influence on the mechanical characteristics of cement-stabilized macadam (CSM) was systematically investigated. Combined with life cycle assessment (LCA), the carbon emission reduction potential was quantitatively evaluated, aiming to improve the toughness of road base materials and promote low-carbon sustainable development. The results demonstrate that when the PA content increases from 0% to 20%, the mechanical strength of CSM gradually decreases, while the toughness presents a steady upward trend, and the maximum carbon emission reduction rate reaches 50.8%. The optimal toughness improvement of 28.39% is obtained at the PA content of 16%. This study clarifies the internal correlation between mechanical behaviors and low-carbon benefits of recycled plastic aggregate, provides reliable technical support for the high-value utilization of waste plastics and the optimization of sustainable road materials, and offers important references for the green and low-carbon transformation of transportation infrastructure.

Keywords: recycled plastic aggregate; cement-stabilized macadam; carbon emission reduction; toughness; sustainable road materials; low carbon

Check for updates

Academic Editor: Maria L. Auad

Received: 23 March 2026
Revised: 27 April 2026
Accepted: 29 April 2026
Published: 2 May 2026

Copyright: © 2026 by the authors. Licensee MDPI, Basel, Switzerland. This article is an open access article distributed under the terms and conditions of the Creative Commons Attribution (CC BY) license.

1. Introduction

Owing to its high mechanical strength, excellent structural integrity and stable structure, cement-stabilized macadam (CSM) is the dominant material for the semi-rigid base of expressways, yet it has inherent defects of poor toughness, insufficient crack resistance and easy early cracking. These issues easily induce pavement structural diseases and significantly raise road maintenance costs [1–3]. Meanwhile, its large-scale application is highly reliant on natural aggregates. However, excessive extraction of natural aggregates will lead to resource depletion, ecological damage and considerable carbon emissions [4–6]. In addition, waste plastic production is escalating continuously with a low resource utilization rate. Traditional disposal methods such as landfilling and incineration have imposed a severe environmental burden [7]. If these plastics are recycled into aggregates to replace

natural aggregates and incorporated into CSM, it can become an effective technical path to resolve the above problems simultaneously, which has important research value [8–11].

Domestic and international scholars have conducted extensive research on flexible-aggregate-modified cement-based materials, including the incorporation of appropriate flexible materials such as fibers, rubber and plastic [12–17]. Ali et al. [18] investigated the feasibility of using plastic coarse aggregates as a partial substitution for natural coarse aggregates in concrete. They found that incorporating PA enhanced the workability of concrete; however, it resulted in a reduction in mechanical performance. Han et al. [19] conducted research on rubberized concrete with varying particle sizes, mixing amounts, and pretreatment approaches, finding that the larger the rubber particles and the lower the mixing amounts, the lower the loss of mechanical properties. Wang et al. [20] added polypropylene (PP) fibers to CSM bases to enhance the crack resistance durability. The findings indicated that the incorporation of 0.1% PP fibers could significantly improve the macroscopic mechanical properties of CSM bases; in particular, the splitting tensile strength (STS) increases by approximately 20%. Meanwhile, the optimal dosage of PP fibers for CSM bases was confirmed. A large number of studies have confirmed the regulatory effect of flexible aggregates on material properties, verified the feasibility of using solid waste in road construction materials, laid a solid foundation for subsequent research, and highlighted the significant application potential of flexible modification technology in road engineering [21–24]. Although existing achievements have shown remarkable effects, there remain three critical gaps. Firstly, most of the current research focused on concrete, and there is a scarcity of systematic experimental and mechanistic studies conducted on CSM modified with PA. Secondly, most studies only prioritized the optimization of a single mechanical property, lacking a collaborative analysis of mechanical performance and carbon emission reduction benefits. Thirdly, no quantitative evaluation system integrating structural performance and low-carbon benefits has been established so far; the coupling mechanism among dosage effects, performance evolution and low-carbon efficiency remains unclear, which is insufficient to support the low-carbon and scientific design of road materials.

Therefore, this study adopted an equal-volume replacement of natural coarse aggregates with plastic aggregates. A gradient content ranging from 0% to 20% was set for the experimental tests. The unconfined compressive strength (UCS), STS, flexural tensile strength (FTS), and toughness indices of the modified mixture were systematically measured. Meanwhile, a carbon emission accounting model was developed based on life cycle assessment (LCA) to quantitatively clarify the intrinsic relationship between the content of PA and the mechanical properties, as well as the carbon emission reduction benefits of CSM. This research clarified the modification and low-carbon efficiency mechanism of waste PA on cement-stabilized macadam, confirmed the optimal dosage range that satisfies both mechanical performance requirements and resource utilization efficiency, and further improved the theoretical system for road base materials modified with solid waste recycled aggregates. The research results provide an experimental basis and technical support for the large-scale and standardized application of waste plastics in road bases, and are of great theoretical significance and engineering value in improving the workability of CSM, promoting the high-value resource utilization of solid waste, and advancing the green and low-carbon transformation of transportation infrastructure.

2. Materials and Methods

Dense structure grading was employed in this test for CSM, in accordance with the Technical Guidelines for the Construction of Highway Road bases (JTG/T F20-2015). The primary raw materials included cement, aggregate, and water. Qinling Grade 32.5 ordinary

Portland cement was used at a dosage of 5% via the external admixture method to prepare CSM. The aggregate was selected from limestone produced by a stone factory in Jingyang County, Shaanxi Province, and classified into three grades according to particle size: 0–5 mm, 5–10 mm, and 10–20 mm. Ordinary tap water was used for mixing. Through standard compaction tests, the optimum water content for each gradation was determined to be 5.53%, with a maximum dry density of 2.42 g/cm^3. The final mix proportions of CSM are presented in Table 1.

Table 1. Mix proportions of cement-stabilized macadam.

Aggregate Specifications (mm)	Mass Percentage	The Mass Percentage (%) Passing Through the Following Square Mesh Sieve (mm)						
		31.5	**19.0**	**9.5**	**4.75**	**2.36**	**0.6**	**0.075**
10–20	28.56%	28.56	25.42	0.07	0.07	0.07	0.05	0.04
5–10	37.13%	37.13	37.13	36.44	1.82	0.10	0.08	0.05
0–5	34.31%	34.31	34.31	34.31	34.19	25.53	14.17	0.55
Synthetic Grading		100	96.86	70.81	36.07	25.70	14.3	0.64
Upper Limit		100	100	90	49	32	20	5
Lower Limit		100	90	60	29	15	6	0

The recycled PA was obtained from a batch of waste plastic rods of the same material, produced by a factory in Xi'an. To eliminate the influence of aggregate shape on the performance of the mixture, the plastic rods were cut and polished to obtain plastic aggregates with consistent shape and a particle size range of 10–20 mm. Fourier-transform infrared spectroscopy (FTIR) confirmed that the material was an acrylonitrile–butadiene–styrene copolymer (ABS). The plastic aggregates used had consistent properties without obvious oxidation or degradation, with a glass transition temperature of approximately 104 °C and negligible crystallinity. The physical properties of PA and natural coarse aggregate are listed in Table 2.

Table 2. Physical properties of recycled plastic aggregate and natural coarse aggregate.

Index	Element	Particle Size (mm)	Apparent Density (g/cm^3)	Deformation Strength (MPa)	Elastic Modulus (GPa)
Plastic	ABS	12	1.03	50	2.2
Coarse Aggregate	Basalt	10–20	2.65	120	60–120

In the test, coarse plastic aggregates with a gradation of 10–20 mm were used to replace 10–20 mm coarse aggregates in equal volume. The replacement ratios were 4%, 8%, 12%, 16%, and 20%, totaling 5 replacement ratios. In addition, a control group without coarse plastic aggregates was set up, meaning there were 6 working conditions in total for this test. Nine parallel samples were prepared for each test group. According to Test Methods of Materials Stabilized with Inorganic Binders for Highway Engineering (JTG 3441-2024), 7 d and 28 d UCS, 7 d and 28 d STS, 28 d FTS, and the toughness of CSM with different plastic coarse aggregate contents were tested [25]. As shown in Figure 1, the specimens were formed by static pressure with a pressure testing machine (Model YAW 1000, Jinan Zhongte Testing Machine Co., Ltd., Jinan, China). Toughness was calculated via energy integration of the load–displacement curve, using displacement and load data recorded by the sensor during the UCS test. "Toughness 1" refers to the pre-cracking stage, and "Toughness 2" represents the rapid crack propagation stage.



Figure 1. Mechanical properties test.

3. Results and Discussion

3.1. Unconfined Compressive Strength

The asphalt pavement base layer acts as the primary load-bearing structure, and its UCS represents a key performance index for CSM. In accordance with the Chinese standard JTG/T F20-2015, the 7-day UCS of CSM for base layers under medium and light traffic conditions shall range from 3 to 5 MPa. As observed in Figure 2, the 7-day UCS of CSM specimens initially increases and then decreases with increasing plastic aggregate (PA) content. The UCS reaches a maximum of 5.966 MPa at the 12% PA content, representing a 4.12% improvement relative to the control group. Accordingly, the optimum replacement ratio is determined to be 12%. This behavior can be explained as follows. At PA contents below 12%, the gradation and filling effect of coarse plastic aggregates is pronounced. Meanwhile, the elastoplastic deformation of coarse PA enables stress absorption and inhibits the initiation of microcracks, leading to a slight improvement in early compressive strength. When the PA content exceeds 12%, the UCS decreases gradually and reaches its minimum at 16%, which is 1.12% lower than that of the control group. This trend indicates that the void-filling effect of fine aggregates approaches saturation, resulting in weak interfacial bonding between plastic aggregates and cement paste, thereby causing a gradual reduction in strength. Notably, the UCS values of all mixtures exceed 5 MPa, meeting the requirements for practical engineering applications. The variation in UCS across all replacement ratios remains within 5.2%, with no statistically significant differences observed. This phenomenon is mainly attributed to the incomplete hydration reaction between coarse plastic aggregates, crushed stone, and cement after a 7-day curing period.

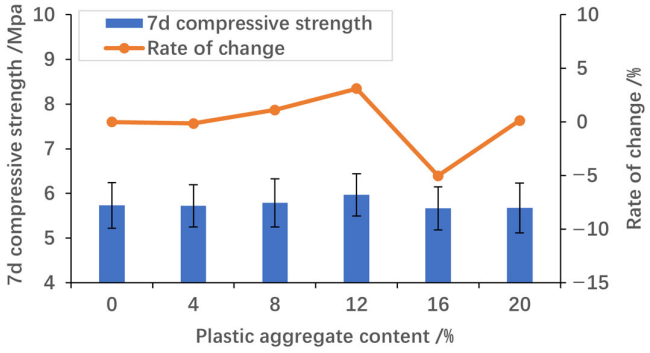


Figure 2. Results of unconfined compression strength at 7 d.

The 28 d UCS and its rate of change for CSM samples are shown in Figure 3. The 28 d UCS decreases monotonically with increasing PA content. The maximum UCS of 10.526 MPa occurs in the control group, while the minimum value of 7.949 MPa appears in the 20% PA group, representing a 24.48% reduction. This indicates that the addition of PA significantly reduces the long-term compressive performance of CSM. This effect arises

mainly from the hydrophobic nature of PA and its weak interfacial bonding with the cement matrix, both of which lower load-transfer efficiency. At higher PA contents, the interfacial transition zone (ITZ) becomes more prominent, further reducing compressive strength. The rate of change in UCS reaches its maximum at the 12% content level, indicating this as the critical turning point. Below this value, strength decreases gradually. By comparing 7 d and 28 d UCS variations, it is found that the 7 d UCS is 4.12% higher than that of the control group, whereas the 28 d strength shows a 14.45% loss. This can be explained by sufficiently complete cement hydration and stabilized microstructure at 28 d age. The weak interfaces between PA and cement paste form a continuous weak network, and the low strength and low elastic modulus of the plastic render it unfavorable for sustained loading. Eventually, the weak interfaces govern the mechanical response, leading to continuous strength degradation.

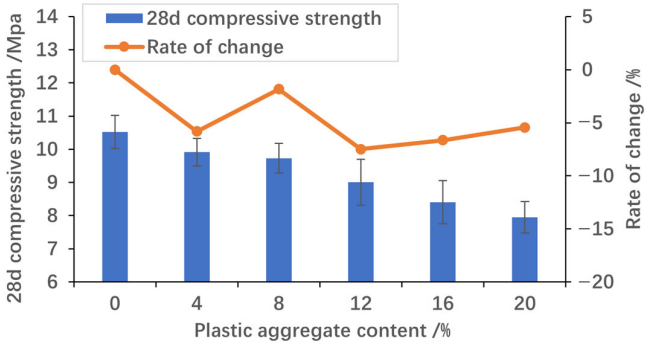


Figure 3. Results of unconfined compression strength at 28 d.

3.2. Splitting Tensile Strength

As shown in Figure 4, the variation in STS of CSM samples with PA content is highly consistent with that of UCS. The 7-day STS rises first and then falls, peaking at 0.484 MPa with a PA content of 16%. An appropriate amount of PA improves early-stage skeleton interlocking and mixture densification, slightly enhancing early cracking resistance and splitting bearing capacity. Nevertheless, this positive effect diminishes over time. The 28-day STS decreases continuously with increasing PA content, dropping to 0.506 MPa at the 20% PA content—a reduction of 22.27%. This is mainly because the low elastic modulus of PA causes severe stress concentration in the ITZ, while its hydrophobicity weakens interfacial bonding and accelerates crack initiation. Compared with the control group, PA significantly suppresses long-term strength growth, leading to an abrupt strength drop at the 20% PA content mark. Therefore, the PA dosage should be strictly limited below this threshold to avoid sharp mechanical degradation in engineering applications.

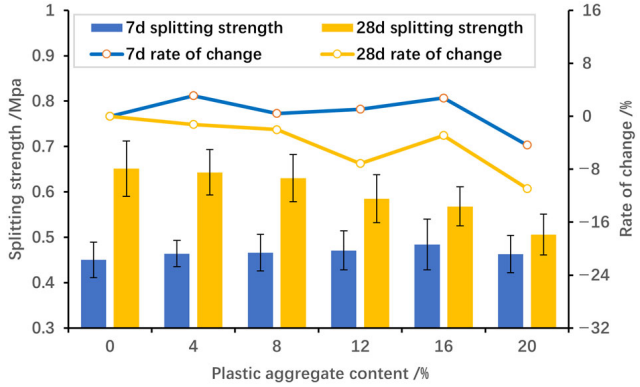


Figure 4. Results of splitting tensile strength at 7 d and 28 d.

3.3. Flexural Tensile Strength

As shown in Figure 5, the 28-day FTS of CSM samples decreases monotonically with increasing PA content, reaching a minimum of 0.67 MPa at 20% PA content—a total reduction of 25.56%. This indicates that incorporating coarse PA continuously degrades the flexural tensile performance of CSM, which is consistent with the variation trends of UCS and STS. For short-term temporary engineering projects, a PA content of 12% to 16% is recommended to maximize solid waste utilization. For road bases under medium and light traffic conditions, PA content should be controlled below 12% to balance waste plastic recycling and the long-term mechanical stability of CSM. For high-grade roads or higher PA dosages, surface modification of PA is required, such as roughening, binder coating, and fiber incorporation. By improving the crack resistance and interfacial bonding strength of the mixture, the adverse effects induced by weak interfaces can be effectively compensated.

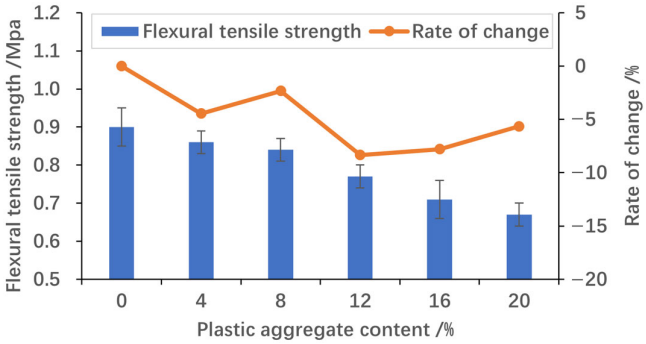


Figure 5. Results of flexural tensile strength at 28 d.

3.4. Toughness

As shown in Figure 6, under a constant load of 30 kN maintained for 30 s, the displacement of compressed specimens increases monotonically with increasing PA content. When the PA content reaches 20%, the displacement of specimens rises from 1.366 mm to 2.494 mm, with an increase of 82.6%, and no specimen fails under the 30 kN load. This is attributed to the elastic nature of plastic, which reduces the overall stiffness and increases the deformation of the mixture as PA content rises. The displacement growth rate also differs significantly. The largest increase of 32.21% occurs in the range from 0% to 4%. The growth rate slows down in the range from 4% to 16%. When the PA content exceeds 16%, the growth rate of displacement returns to 16.43%. The analysis of the cause reveals that under a low substitution rate, the PA damages the cementation network of cement paste, leading to a sudden drop in stiffness. At a medium replacement ratio, the filling effect and constraint effect of fine aggregate are balanced, while at a high replacement ratio, weak interfaces form a continuous weak network leading to rapid deformation. In summary, the addition of coarse PA decreases stiffness and improves the plastic deformation capacity of CSM. In engineering applications, it is recommended to control the PA content below 16% to prevent uncontrolled deformation.

The load–displacement curves of CSM specimens with varying PA contents are presented in Figure 7. These curves can be categorized into two distinct stages. In the first stage (OA), the load and displacement exhibit a linear relationship, suggesting that initial cracks remain stationary during loading. In the second stage (AB), rapid crack propagation occurs, leading to abrupt failure of the specimen. As the PA content increases from 0% to 20%, the maximum load of CSM decreases from 86.88 kN to 59.23 kN, while the peak displacement increases from 2.16 mm to 3.53 mm. This indicates that higher PA content results in greater displacement under the same load and lower load-carrying capacity at the same displacement. Overall, coarse PA contributes to the dispersion and cushioning of

external loads, thereby improving force transfer efficiency within the CSM mixture and enhancing its load deformation capacity.

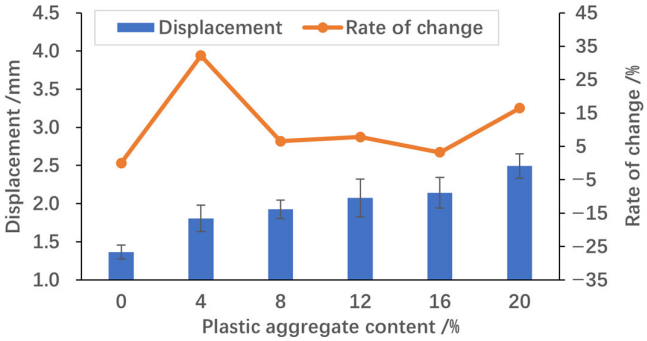


Figure 6. Changing trends of the displacement of the CSM specimens loaded with 30 kN for 30 s.

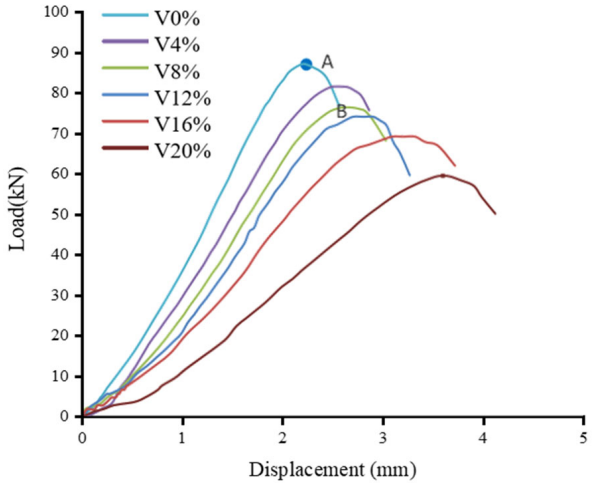


Figure 7. Load–displacement curves of different proportions of coarse plastic aggregates. **Point A**: The end of the pre-cracking stage (OA segment), representing the peak load and the onset of unstable crack propagation. **Point B**: A key feature point in the rapid crack propagation stage (AB segment), indicating the specimen's accelerated damage and failure after the peak load.

The effect of coarse PA on the toughness of CSM was evaluated by the area enclosed by the load–displacement curve and the x-axis, as summarized in Figure 8. Here, Toughness 1 describes the stage before cracking and stable propagation and Toughness 2 describes rapid crack growth. It is revealed that the incorporation of coarse PA effectively improves the toughness of CSM, with all modified specimens exhibiting higher toughness values than the control group. This improvement can be attributed to the inherent elastic deformation of plastic particles, which enable additional energy absorption and stress relaxation under loading, thus reinforcing the overall toughness of the composite. Toughness 1 first increases and then decreases with rising PA content, while Toughness 2 shows a fluctuating but overall increasing tendency. Both toughness indices reach their maxima at 16% PA, suggesting that this dosage optimizes the toughening efficiency. Excessive PA beyond 16% tends to generate continuous weak interfacial zones, which deteriorate structural integrity and reduce energy absorption capacity. Accordingly, the toughening effect is most pronounced at a PA content of 16%. For engineering applications, controlling the PA content within 16% is recommended to improve crack resistance and ensure favorable long-term mechanical performance.

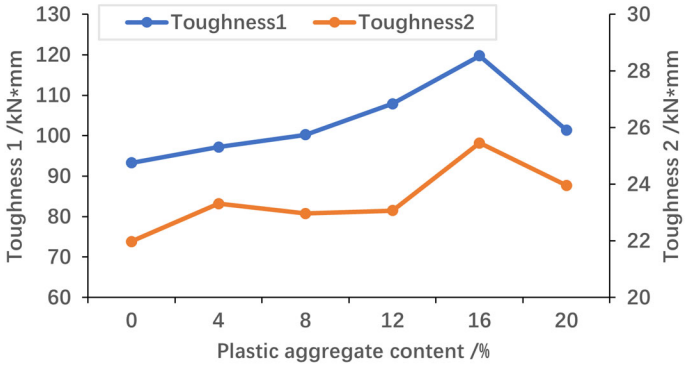


Figure 8. Toughness of the CSM specimens under different plastic aggregate contents.

The distribution of coarse plastic aggregates in fractured specimens with different PA contents is shown in Figure 9. Coarse plastic aggregates can be observed at the failure interface of the specimens. These plastic particles remain intact without crushing, but most are pulled out from the matrix, indicating that the bonding strength between coarse plastic aggregates and the surrounding cementitious matrix is relatively weak, making this region prone to crack initiation. In addition, the number of plastic aggregates at the failure interface increases with increasing PA content, as marked by the red circles in the figure. This implies that a higher PA content introduces more weak interfacial zones within the mixture. It is also observed that the distribution of coarse plastic aggregates becomes increasingly nonuniform as the PA content rises.

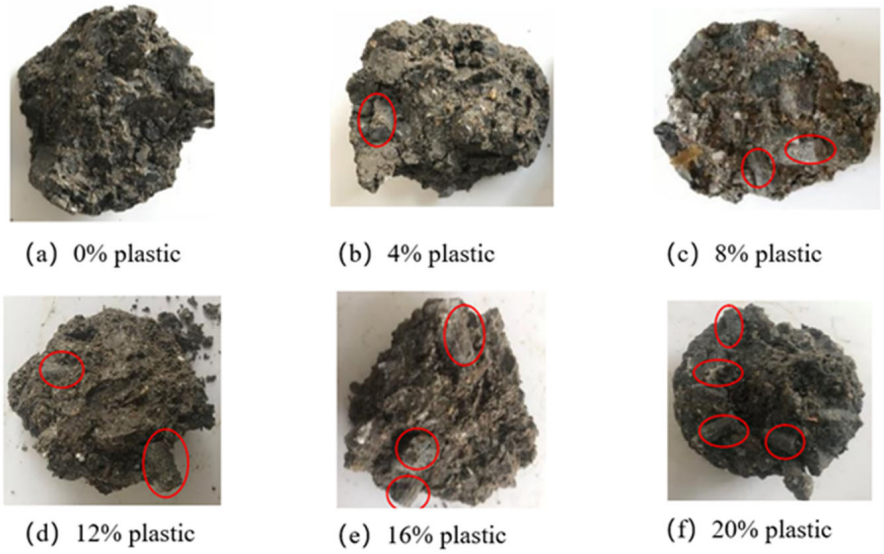


Figure 9. Distribution of coarse plastic aggregates in the crushed samples.

Therefore, the mechanisms by which the addition of coarse PA reduces the UCS, STS, and FTS of CSM can be summarized as follows. Firstly, the weak interfacial bonding between cement paste and the surface of coarse PA undermines the overall integrity and strength of the mixture. Secondly, the hydrophobic characteristic of coarse PA restricts moisture availability in its vicinity, giving rise to weak physical and chemical interactions with cement hydration products that hinder the hydration process. Lastly, the interlocking effect among aggregate particles, which is critical to the strength of CSM, is weakened by the regular particle shape and low friction coefficient of PA, thus inhibiting effective interlocking with adjacent fine and coarse aggregates.

4. Carbon Emission Reduction Analysis

4.1. Carbon Emission Accounting

This study adopts the theory of LCA and uses the carbon emission factor method to calculate the carbon emissions and carbon reduction benefits of CSM mixtures. The functional unit is set as 1 m^3 of CSM mixture. The accounting scope strictly focuses on the whole process of raw material production and mixture preparation in the upstream stage, up to the uniform mixing of the mixture in the laboratory, excluding subsequent stages such as on-site construction and paving, service period, and waste disposal. All accounting items refer to the carbon emissions directly generated within this boundary. Two core processes are included within the accounting boundary. First is the raw material production stage, covering the production, processing, crushing, sieving, and short-distance transportation of four materials: Qinling P·C 32.5 cement, limestone coarse aggregate, recycled ABS plastic aggregate, and mixing water. The carbon emissions are the direct emissions of each material. Second is the mixture preparation stage, in which only the carbon emissions from industrial electricity consumption for laboratory mixture mixing are counted, corresponding to the power consumed during the operation of the mixer. The accounting process strictly follows the principles of consistency, directness, and relevance: the accounting boundaries are completely consistent between the control group and each experimental group, and all included carbon emission sources are directly related to the production and preparation of the mixture, ensuring the objectivity and accuracy of the accounting results [26].

This study has certain limitations, as the LCA accounting boundary does not cover the stages of construction, transportation, service, and end-of-life disposal. If these stages were included, the total carbon emissions would increase due to energy consumption in construction and transportation. The recycled ABS plastic aggregate has stable performance and no obvious adverse effect on the long-term service performance and waste treatment mode of the material. The carbon reduction benefits in the full life cycle are basically consistent with the calculated results in this paper, and may even be further improved due to the recyclable characteristics of plastic aggregate.

Based on the above definitions, a carbon emission accounting equation is established as Equation (1). In this equation, E_o represent the total carbon emission of 1 m^3 mixture (kg CO_2/m^3); m_c, m_a, m_p, and m_w represent the mass contents of cement, limestone aggregate, waste PA, and mixing water in 1 m^3 mixture, respectively (kg/m^3); and f_c, f_a, and f_w represent the carbon emission factors of the corresponding materials (kg CO_2/kg). Specifically, f_c is taken as 0.604 kg CO_2/kg, f_a is taken as 0.0044 kg CO_2/kg, and f_w is taken as 0.000168 kg CO_2/kg. f_p denotes the net life-cycle carbon emission reduction factor of recycled ABS plastics, which is assigned a value of −0.8 kg CO_2/kg. This is a widely accepted LCA-based net emission reduction value in the industry, covering both direct production emissions and the emission reduction benefit from replacing virgin plastic; E_{ip} represents the carbon emissions from electricity consumption during the production of the 1 m^3 mixture. All the above carbon emission factors and parameters were obtained from the Standard for Building Carbon Emission Calculation (GB/T 51366-2019) and the China Life Cycle Database (CLCD).

$$E_o = m_c \times f_c + m_a \times f_a + m_p \times f_p + m_w \times f_w + E_{ip} \quad (1)$$

The carbon emissions from electricity consumption in 1 m^3 mixture production are calculated by Equation (2). In this equation, P represents the power of the mixer (kW); t

represents the mixing time (min); f_{ip} represents the carbon emission factor for industrial electricity, taken as 0.58 kg CO_2/(KW·h); and V represents the per-batch output volume.

$$E_{ip} = P \times t/60 \times f_{ip}/V \quad (2)$$

The carbon emission reduction is given by Equation (3). In this equation, E_b represents the carbon emission of the control group. E_t represents the carbon emission of each test group.

$$\Delta E = E_b - E_t \quad (3)$$

The carbon emission reduction rate is given by Equation (4).

$$\eta = \frac{\Delta E}{E_b} \times 100\% \quad (4)$$

The carbon emission intensity is given by Equation (5). In this equation, f_{cs} represents the compressive strength.

$$E_s = E_o/f_{cs} \quad (5)$$

4.2. Analysis of Carbon Emission Reduction Effect

This section uses the LCA method to analyze variation patterns of the carbon reduction volume, carbon reduction rate, and carbon reduction intensity of the mixture. Experiments replace coarse aggregates with different amounts of plastic coarse aggregates in equal volumes, and the carbon reduction effects of recycled plastic aggregates are shown in Figure 10.

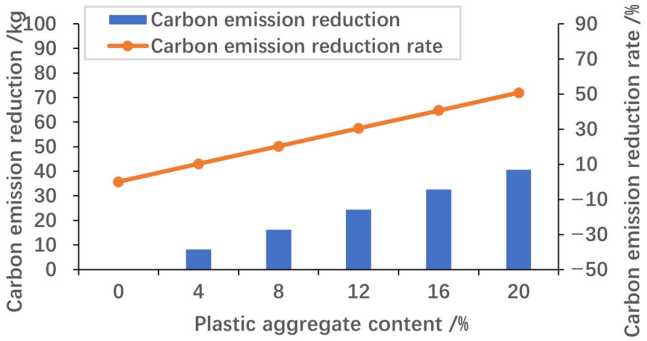


Figure 10. Carbon emission reduction and carbon reduction rate of CSM with different plastic aggregate contents.

As shown in Figure 10, the carbon reduction of the mixture increases linearly with increasing PA content. At a content of 4%, the amount of carbon reduced is 8.14 kg with a carbon reduction rate of 10.16%, whereas a 20% PA content increases the carbon reduction amount to 40.68 kg, corresponding to a reduction rate of 50.8%. There exists a positive correlation between PA content and carbon reduction efficiency. For each 4% increase in PA content, the carbon reduction rate increases by approximately 10%, and the carbon reduction amount increases by about 8 kg. This is attributed to the dual emission reduction mechanism of plastic recycling. Replacing coarse aggregates with an equal volume of recycled plastics directly reduces carbon emissions from mining and crushing natural aggregates, as well as virgin plastic production. Moreover, the carbon reduction effect becomes increasingly prominent with higher PA content. This demonstrates the significant carbon emission reduction potential of recycled plastic aggregates in road base materials and provides a quantitative reference for the design of high-volume solid waste replacement in engineering practice. Combined with the variation trend of UCS, the optimal PA dosage

is suggested to be 8–12%, within which the reduction in mechanical properties is less than 14.45%. This range is suitable for road bases under medium and light traffic loads, and achieves a favorable balance between the mechanical performance and low-carbon benefits of the mixture.

Figure 11 shows that the carbon emission intensity decreases linearly with the increase in PA content. As the PA content rises from 0% to 20%, the carbon emission intensity decreases from 7.67 to 4.96, representing a reduction of 35.3%. This means that the recycled plastic aggregates not only reduce the carbon emissions per unit volume of mixture but also improve the low-carbon benefits per unit of mechanical strength. The comprehensive performance balancing low-carbon characteristics and mechanical properties is gradually optimized with increasing PA content. The reduction in carbon emission intensity is consistent with the increasing carbon emission reduction rate shown in Figure 10, thus confirming the net emission reduction effect of recycled plastics from performance and emissions. This directly addresses the critical question of "How much can carbon emissions be reduced using recycled plastic aggregates under the same mechanical strength requirements?", thereby providing a vital quantitative basis for optimizing the mechanical properties of road engineering and pursuing low-carbon development goals.

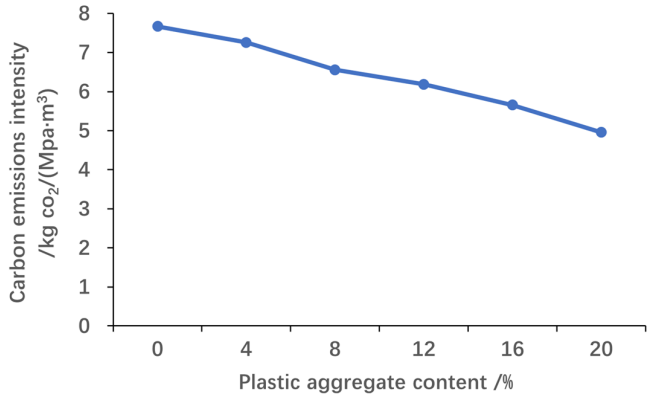


Figure 11. Carbon emission reduction intensity of CSM with different plastic aggregate contents.

5. Conclusions

This paper studies the effect of different proportions of coarse plastic aggregates replacing coarse aggregates in equal quantity on the mechanical properties of CSM mixtures, and evaluates 7 d and 28 d compressive strength, splitting strength, flexural tensile strength, toughness and carbon emission properties of CSM modified by plastic aggregate. The main conclusions are as follows.

(1) Compared with ordinary CSM, adding a small proportion of coarse plastic aggregates slightly increases the 7 d compressive strength, splitting strength, and flexural tensile strength of the material. At the optimal dosage of 12%, the overall improvement in mechanical properties remains below 8%.

(2) With the increase in PA content, the 28 d compressive strength, splitting strength, and flexural tensile strength of CSM exhibit a gradual decreasing trend. When the PA content is below 16%, the degradation in overall mechanical properties is less than 22%, making the CSM mixture applicable to short-term temporary road projects. This scheme enables the high-value resource utilization of waste plastics while satisfying basic mechanical performance requirements. For the base layer of heavy traffic roads, it is recommended that the PA content is less than 8%, and the reduction in overall mechanical property is less than 8%, which can balance environmental benefits and engineering performance. For medium and light traffic road base layers, the PA content can be relaxed to 12%, with a mechanical property reduction of 14.45%.

(3) The toughness of CSM shows a trend of continuous increase first and then peak decline with the increase in PA content, and the toughness values of all test groups are higher than that of the control group. The results demonstrate that adding plastic coarse aggregates can enhance the toughness of CSM. At the optimal dosage of 16%, the maximum improvement in toughness reaches 28.39%. It is recommended in engineering practice to control the PA content below 16% to improve the crack resistance and toughness of the material.

(4) The equal-volume replacement of natural coarse aggregate with recycled PA can achieve remarkable carbon emission reduction results, and the carbon reduction effect is linearly and positively correlated with the PA content. Under the test conditions, the carbon reduction rate of the CSM mixture exceeds 50% at a PA content of 20%, and the carbon emission intensity decreases by 35.3%. It is shown that recycled plastic aggregates can reduce emissions from road base materials and improve the resource utilization value of waste plastics. The optimal dosage range of PA is 8% to 12%, within which the mechanical properties and low-carbon benefits of the CSM mixture can be guaranteed simultaneously.

(5) The utilization of recycled plastic aggregates can enhance the combined benefits of low-carbon performance and mechanical properties of the CSM mixture. The carbon emission per unit strength decreases from 7.67 to 4.96, with a reduction of 35.3%. This means that the incorporation of recycled plastic aggregates reduces carbon emissions without compromising carbon emission efficiency per unit of mechanical strength. Instead, it enhances the low-carbon cost-effectiveness of the material, and provides a crucial quantitative foundation for the optimization of mechanical properties and low-carbon design in road engineering.

Author Contributions: Conceptualization, M.C. and W.G.; Methodology, H.G., Y.Y., W.G. and C.C.; Validation, M.C.; Formal analysis, H.G., M.C., W.G. and C.C.; Investigation, M.C., Y.Y., W.G. and C.C.; Resources, Y.Y.; Data curation, H.G. and C.C.; Writing—original draft, H.G.; Writing—review and editing, S.C. and Y.Y.; Supervision, S.C.; Project administration, S.C. and Y.Y.; Funding acquisition, S.C. All authors have read and agreed to the published version of the manuscript.

Funding: This work was supported by the Qinchuangyuan "Scientist + Engineer" Project of Shaanxi Province (Grant No. 2025QCY-KXJ-136).

Institutional Review Board Statement: Not applicable.

Informed Consent Statement: Not applicable.

Data Availability Statement: The original contributions presented in this study are included in the article. Further inquiries can be directed to the corresponding author.

Conflicts of Interest: The authors declare no conflicts of interest.

Abbreviations

The following abbreviations are used in this manuscript:

PA	Plastic aggregate
CSM	Cement-stabilized macadam
LCA	Life cycle assessment
UCS	Unconfined compressive strength
PP	Polypropylene
STS	Splitting tensile strength
FTS	Flexural tensile strength

References

1. Xia, X.; Han, D.D.; Ma, Y.C.; Zhao, Y.; Tang, D.; Chen, Y. Experiment investigation on mix proportion optimization design of anti-cracking stone filled with cement stabilized macadam. *Constr. Build. Mater.* **2023**, *393*, 132136. [CrossRef]
2. Pan, Y.Y.; Chen, A.Q.; Lin, M.; Ma, Y.; Zhao, Y. Microscale characterization of an anti-cracking stone base course filled with cement stabilized macadam. *Constr. Build. Mater.* **2024**, *425*, 136037. [CrossRef]
3. Yang, X.K.; Wu, S.P.; Chen, B.Y.; Ye, G.; Xu, S. Development of a sustainable stabilized macadam road base using steel slag as supplementary cementitious material. *Constr. Build. Mater.* **2024**, *449*, 138566. [CrossRef]
4. Zhao, M.Z.; Liu, H.; Wang, Q.L.; Wang, M.; Chen, Z.; Wang, X. Performance enhancement and mechanism analysis of low-carbon cement-stabilized macadam based on vibratory mixing method. *Case Stud. Constr. Mater.* **2025**, *23*, e04990. [CrossRef]
5. Yuan, L.Q.; Liu, L.P.; He, M.; Liu, Q.; Cheng, H.; Sun, L.; Guo, L. Sustainable pavement solutions: Performance enhancement using high-dosage unequal-sized feldspar powder as a replacement for natural aggregates in cement stabilized macadam bases. *Constr. Build. Mater.* **2025**, *459*, 139620. [CrossRef]
6. Wang, J.J.; Ding, Y.J.; Zhou, Y.X.; Wei, W.; Wang, Y. Municipal solid waste incineration bottom ash recycling assessment: Carbon emission analysis of bottom ash applied to pavement materials. *Constr. Build. Mater.* **2024**, *421*, 135774. [CrossRef]
7. Chen, G.Y.; Li, J.Y.; Sun, Y.N.; Wang, Z.; Leeke, G.A.; Moretti, C.; Cheng, Z.; Wang, Y.; Li, N.; Mu, L.; et al. Replacing Traditional Plastics with Biodegradable Plastics: Impact on Carbon Emissions. *Engineering* **2024**, *32*, 152–162. [CrossRef]
8. Hu, K.; Gillani, S.T.A.; Tao, X.H.; Tariq, J.; Chen, D. Eco-friendly construction: Integrating demolition waste into concrete masonry blocks for sustainable development. *Constr. Build. Mater.* **2025**, *460*, 139797. [CrossRef]
9. Salgado, F.D.; Silva, F.D. Recycled aggregates from construction and demolition waste towards an application on structural concrete: A review. *J. Build. Eng.* **2022**, *52*, 104452. [CrossRef]
10. Soharu, A.; Bp, N.; Vaid, K. Influence of using waste plastic as coarse aggregates-based sustainable concrete. In *Proceedings of the Institution of Civil Engineers-Waste and Resource Management*; Emerald Publishing Limited: Leeds, UK, 2026; Volume 179, pp. 45–54. [CrossRef]
11. Ma, X.S.; Hu, H.B.; Luo, Y.; Yao, W.; Wei, Y.; She, A. A carbon footprint assessment for usage of recycled aggregate and supplementary cementitious materials for sustainable concrete: A life-cycle perspective in China. *J. Clean. Prod.* **2025**, *490*, 144772. [CrossRef]
12. Tao, R.; Cheng, X.J.; Jin, Y.; Qiao, J.; Zhang, X.; Kim, D.; Liu, J. Mechanical properties of double-solid waste cement stabilized Macadam. *Sci. Rep.* **2025**, *15*, 4425. [CrossRef] [PubMed]
13. Yuan, L.Q.; Liu, L.P.; Sun, L.J.; Liu, Q.; Li, M.; Liu, N. Feasibility study of lithium slag as cementitious material with high-content application in cement stabilized macadam bases. *Constr. Build. Mater.* **2024**, *457*, 139224. [CrossRef]
14. Xiao, R.; Nie, Q.K.; He, J.X.; Lu, H.; Shen, Z.; Huang, B. Utilizing lowly-reactive coal gasification fly ash (CGFA) to stabilize aggregate bases. *J. Clean. Prod.* **2022**, *370*, 133320. [CrossRef]
15. Li, H.B.; Yan, P.F.; Tian, J.C.; Sun, H.; Yin, J. Study on Mechanical and Frost Resistance Properties of Slag and Macadam Stabilized with Cement and Fly Ash. *Materials* **2021**, *14*, 7241. [CrossRef] [PubMed]
16. Guo, Y.C.; Yao, C.; Shen, A.Q.; Chen, Q.; Wei, Z.; Yang, X. Feasibility of rapid-regeneration utilization in situ for waste cement-stabilized macadam. *J. Clean. Prod.* **2020**, *263*, 121452. [CrossRef]
17. Chi, M.X.; Shen, Z.Z.; Chen, S.B.; Yao, Y.; Shen, J.; Li, C.; Yan, Q. Influence of plastic aggregate geometry on strength properties of cement-stabilized macadam. *Sci. Rep.* **2023**, *13*, 15270. [CrossRef]
18. Ali, K.; Saingam, P.; Qureshi, M.I.; Saleem, S.; Nawaz, A.; Mehmood, T.; Maqsoom, A.; Malik, M.W.; Suparp, S. Influence of Recycled Plastic Incorporation as Coarse Aggregates on Concrete Properties. *Sustainability* **2023**, *15*, 5937. [CrossRef]
19. Han, X.Y.; Wang, L.; Chen, A.J.; Feng, L.; Ji, Y.; Wang, Z.; Gao, Z.; Li, K.; Yuan, Q.; Xia, X.; et al. Experimental and analytical evaluation of mechanical properties of rubberized concrete incorporating waste tire crumb rubber. *Case Stud. Constr. Mater.* **2025**, *23*, e04970. [CrossRef]
20. Wang, Z.L.; Huang, W.Y.; Zhao, J.L.; Kong, L.; Jiang, S.; Xia, S.; Ren, D.; Tian, G. The Performance Evaluation of Crack Resistance in Cement Stabilized Macadam Base Reinforced with Polypropylene Fibers Based on DIC Technology. *Int. J. Pavement Res. Technol.* **2024**, *19*, 733–747. [CrossRef]
21. Yan, S.; Lu, H.A.; Zhou, Z.; Dong, Q.; Chen, X.; Wang, X. A polymer latex modified superfine cement grouting material for cement-stabilized macadam—Experimental and simulation study. *Constr. Build. Mater.* **2024**, *413*, 134893. [CrossRef]
22. Wang, G.; Zhuang, Y.H.; Song, L.B.; He, Z.; Zhang, J.; Zhou, H. Mechanical properties and failure mechanism of fiber-reinforced concrete materials: Effects of fiber type and content. *Constr. Build. Mater.* **2025**, *465*, 140190. [CrossRef]
23. Zhang, Y.; Zhang, S.Q.; Jiang, X.; Zhao, W.; Wang, Y.; Zhu, P.; Yan, Z.; Zhu, H. Uniaxial tensile properties of multi-scale fiber reinforced rubberized concrete after exposure to elevated temperatures. *J. Clean. Prod.* **2023**, *389*, 136068. [CrossRef]
24. Iqbal, H.W.; Hamcumpai, K.; Nuaklong, P.; Likitlersuang, S.; Chintanapakdee, C.; Wijeyewickrema, A.C. Effect of graphene nanoplatelets on engineering properties of fly ash-based geopolymer concrete containing crumb rubber and its optimization using response surface methodology. *J. Build. Eng.* **2023**, *75*, 107024. [CrossRef]

25. Cai, P.C.; Mao, X.S.; Lai, X.Y.; Wu, Q. Influence mechanism of brick-concrete ratio on the mechanical properties and water permeability of recycled aggregate pervious concrete: Macroscopic and mesoscopic insights. *Constr. Build. Mater.* **2025**, *467*, 140379. [CrossRef]
26. Qiang, Z.M.; Nan, Q.; Chi, W.C.; Qin, Y.; Yang, S.; Zhu, W.; Wu, W. Recycling packaging waste from residual waste reduces greenhouse gas emissions. *J. Environ. Manag.* **2024**, *371*, 123028. [CrossRef]

Disclaimer/Publisher's Note: The statements, opinions and data contained in all publications are solely those of the individual author(s) and contributor(s) and not of MDPI and/or the editor(s). MDPI and/or the editor(s) disclaim responsibility for any injury to people or property resulting from any ideas, methods, instructions or products referred to in the content.